

ARTICLE

Lung tumor MHCII immunity depends on in situ antigen presentation by fibroblasts

Dimitra Kerdidani¹, Emmanouil Aerakis¹, Kleio-Maria Verrou², Ilias Angelidis¹, Katerina Douka¹, Maria-Anna Maniou¹, Petros Stamoulis¹, Katerina Goudevenou¹, Alejandro Prados¹, Christos Tzaferis^{1,2}, Vasileios Ntafis³, Ioannis Vamvakaris⁴, Evangelos Kaniaris⁵, Konstantinos Vachlas⁶, Evangelos Sepsas⁶, Anastasios Koutsopoulos⁷, Konstantinos Potaris⁶, and Maria Tsoumakidou^{1,2}

A key unknown of the functional space in tumor immunity is whether CD4 T cells depend on intratumoral MHCII cancer antigen recognition. MHCII-expressing, antigen-presenting cancer-associated fibroblasts (apCAFs) have been found in breast and pancreatic tumors and are considered to be immunosuppressive. This analysis shows that antigen-presenting fibroblasts are frequent in human lung non-small cell carcinomas, where they seem to actively promote rather than suppress MHCII immunity. Lung apCAFs directly activated the TCRs of effector CD4 T cells and at the same time produced C1q, which acted on T cell C1qbp to rescue them from apoptosis. Fibroblast-specific MHCII or C1q deletion impaired CD4 T cell immunity and accelerated tumor growth, while inducing C1qbp in adoptively transferred CD4 T cells expanded their numbers and reduced tumors. Collectively, we have characterized in the lungs a subset of antigen-presenting fibroblasts with tumor-suppressive properties and propose that cancer immunotherapies might be strongly dependent on in situ MHCII antigen presentation.

Introduction

The series of immunological events that takes place between tumors and tumor-draining LNs forms a cyclic trajectory that is being referred to as the cancer-immunity cycle (Chen and Mellman, 2013). In the first step of these events, tumor antigens are carried to the tumor-draining LNs and are partly transferred to resident dendritic cells (DCs; Ruhland et al., 2020). In LNs, migratory and resident DCs present their antigenic cargo to antigen-inexperienced (naive) T cells, which become differentiated effector cells that egress from LNs and enter tumors. In tumors, CD8 cells exhibit direct killing activity against cancer cells, but they are seriously dependent on CD4 T cells for function and transition to memory cells (Ahrends et al., 2019; Binnewies et al., 2019; Śledzińska et al., 2020; Zander et al., 2019; Bos and Sherman, 2010; Schietinger et al., 2010). Although our current understanding of the functional space in the cancer-immunity cycle is that MHCII cancer antigen presentation primarily occurs in LNs, the contribution of in situ cancer antigen presentation has not been ruled out (Dammeijer et al., 2020; Oh et al., 2020).

A few studies have directly addressed the role of peripheral antigen presentation in CD4 T cell responses (Dammeijer et al., 2020; Doebis et al., 2011; Low et al., 2020; McLachlan and

Jenkins, 2007; Schøller et al., 2019). In cancer, three lines of evidence support that the TCRs are stimulated in situ within solid tumors. First, the CD4 TCR repertoire is regionally shaped by the local neoantigen load (Joshi et al., 2019). Second, stemlike CD8 T cells reside in dense MHCII-expressing cell niches within tumors (Jansen et al., 2019). Third, right flank tumors that differ only in one MHCII neoantigen with left flank tumors are infiltrated by higher numbers of neoantigen-specific CD4⁺ T cells (Alspach et al., 2019). DCs are scarce and immature within solid tumors and are generally considered to exert their primary effects in LNs (Dammeijer et al., 2020; Ferris et al., 2020; Maier et al., 2020; Ruhland et al., 2020; Oh et al., 2020). Because structural tissue cells greatly outnumber professional antigen-presenting cells, express immune genes (Krausgruber et al., 2020), and can be induced to present antigens (Koyama et al., 2019; Low et al., 2020), we hypothesized that they are required for local antigen presentation and anti-tumor immunity.

Fibroblasts are largely considered to be immunosuppressive cells (Biffi and Tuveson, 2021). Accordingly, the recently identified MHCII⁺ antigen-presenting cancer-associated fibroblasts (apCAFs) in pancreatic adenocarcinoma (PDAC) and breast carcinoma (BC) are presumed to induce immune tolerance

¹Institute of Bioinnovation, Biomedical Sciences Research Center “Alexander Fleming,” Vari, Greece; ²Greek Research Infrastructure for Personalized Medicine, Medical School, National and Kapodistrian University of Athens, Athens, Greece; ³Animal House Facility, Biomedical Sciences Research Center “Alexander Fleming,” Vari, Greece; ⁴Department of Pathology, Sotiria Chest Hospital, Athens, Greece; ⁵Department of Respiratory Medicine, Sotiria Chest Hospital, Athens, Greece; ⁶Department of Thoracic Surgery, Sotiria Chest Hospital, Athens, Greece; ⁷Department of Pathology, Medical School, University of Crete, Crete, Greece.

Correspondence to Maria Tsoumakidou: tsoumakidou@fleming.gr.

© 2022 Kerdidani et al. This article is distributed under the terms of an Attribution–Noncommercial–Share Alike–No Mirror Sites license for the first six months after the publication date (see <http://www.rupress.org/terms/>). After six months it is available under a Creative Commons License (Attribution–Noncommercial–Share Alike 4.0 International license, as described at <https://creativecommons.org/licenses/by-nc-sa/4.0/>).

(Dominguez et al., 2020; Kieffer et al., 2020; Elyada et al., 2019; Friedman et al., 2020; Sebastian et al., 2020). Here, we show that MHCII-expressing fibroblasts are frequently found in lung non-small cell carcinomas and that they anatomically define areas of high rather than low CD4 T cell density. In orthotopic murine models of lung cancer, fibroblast-specific targeted ablation of MHCII impaired local immunity and accelerated tumor growth. Human and murine apCAFs directly activated the TCRs of effector CD4 T cells and, in parallel, protected them from apoptosis via the C1q receptor C1qbp, while C1qbp over-expression expanded the pool of adoptively transferred CD4 T cells in tumors and reduced tumor burden. Our studies identify and characterize lung apCAFs as tumor-suppressive cells and propose a new conceptual framework under which tumor MHCII immunity can be seen: CD4 T cells require in situ antigen presentation within tumors for effective MHCII immunity to occur.

Results

apCAFs activate adjacent CD4 T cells within human lung tumors

To elaborate on the fibroblastic identity of MHCII⁺ non-hematopoietic cells, we enzymatically dispersed primary human tumors and analyzed known mesenchymal markers by FACS (Fig. 1 A). MHCII⁺Lin⁻CAFs (apCAFs) were phenotypically similar to their MHCII⁻ counterparts and largely coexpressed FAP, PDGFR α , and Podoplanin. Vimentin was expressed at variable levels, while α SMA was lowly expressed (Fig. 1 A). Accordingly, two-dimensional (2D) visualization of lineage⁻ cells in t-distributed stochastic neighbor embedding (t-SNE) plots (input all mesenchymal markers) confirmed that apCAFs do not cluster separately from MHCII⁻ cancer-associated fibroblasts (CAFs). To determine the spatial relationship between apCAFs and CD4 T cells, we analyzed whole-tumor tissue sections by immunofluorescence staining. apCAFs were identified as CD45⁻ cells that coexpressed MHCII and FAP. We noticed that FACS had impressively underestimated the frequencies of fibroblasts compared with imaging. This discrepancy likely reflected differences in detachment efficiency of different cell types following tissue digestion, with fibroblasts being more adherent to the extracellular matrix (ECM) than immune cells and thus more difficult to disconnect. Quantitative analysis showed similar densities of intratumoral MHCII⁺FAP⁺CD45⁻ relative to MHCII⁺FAP⁻CD45⁺ hematopoietic antigen-presenting cells, indicating a physiologically relevant abundance of apCAFs. CD4⁺ T cells accumulated in dense apCAF regions and were identified closer to apCAFs rather than MHCII⁺FAP⁻CD45⁺ cells (Fig. 1 B). We interrogated whether we could identify MHCII fibroblasts in healthy lungs. To rule out the possibility of contamination by non-fibroblastic cell populations, we gated fibroblasts as FSC-A^{high}Lin⁻FAP⁺ cells. MHCII was expressed by a subset of normal lung fibroblasts, but it was more frequently detected in CAFs (Fig. 1 C). Collectively, the above data suggest that the tumor microenvironment drives antigen presentation in fibroblasts and that apCAFs create functional immunological spots within lung tumors that might sustain CD4 T cell populations.

Spatial heterogeneity of T cell clones suggests regional activation by neighboring antigen-presenting cells that present their cognate antigens (Joshi et al., 2019). We reasoned that apCAFs directly presented cancer MHCII peptides to adjacent CD4 T cells. To test this, we co-cultured primary human CD4 T cells and FAP⁺ CAFs, purified from the same lung tumor fragment, and assessed phosphorylation of the key TCR/CD28-signaling node, mTOR (Fig. 1 D). Primary cell phenotypes are dramatically altered once they are isolated and cultured. To avoid this bias, we used freshly FACS-sorted primary tumor fibroblasts and freshly sorted autologous primary tumor-infiltrating T cells for all our co-cultures. We used the bulk of CAFs rather than MHCII⁺ CAFs to avoid blocking TCR recognition and did not supplement the culture medium with exogenous cytokines. Under these stringent conditions, ~1 in 10 intratumoral T cells responded to direct CAF contact by mTOR phosphorylation and CD44 up-regulation, and these effects were abolished with MHCII blockade (Fig. 1 D). Control co-cultures of apCAF-depleted CAFs and CD4 T cells confirmed the dependence of CD4 T cell activation on the apCAF fraction of bulk CAFs (Fig. S1). Thus, human apCAFs acquire exogenous peptides within tumors in vivo and can directly prime adjacent CD4 T cells ex vivo.

apCAFs are detected in tumors of IFN- γ -sufficient mice

To assess whether apCAFs were present in murine tissues, we analyzed two models of orthotopic lung cancer and one metastatic. We inoculated one commercially available Lewis Lung Carcinoma (LLC) cell line (LLC^{mCherry}) or an autochthonous cancer cell line (CULA^{zsGreen}) in the left lung lobe of syngeneic mice or injected melanoma cells (B16F10^{mCherry}) in the tail vein of mice. Tumors were digested and subjected to FACS analysis. Intratumoral FSC-A^{high}CD45⁻EpCAM⁻CD31⁻IAb(MHCII)⁺ non-cancer cells coexpressed Podoplanin and PDGFR α , but not α SMA (Fig. 2 A). Murine FAP antibodies showed nonspecific and unreliable staining and were thus excluded from the analysis. Similar to human apCAFs, 2D visualization of all non-cancer lineage⁻ cells in t-SNE plots indicated that apCAFs are admixed with MHCII⁻ CAFs. Immunofluorescence staining detected MHCII⁺Podoplanin⁺ cells within the tumor bed (Fig. 2 A). Similar to what we had observed in humans, MHCII was more frequently expressed by CAFs relative to healthy lung fibroblasts (Fig. 2 B). To determine whether fibroblasts depended on IFN- γ for MHCII expression, we inoculated LLC cells in the lungs of IL-12 p35^{-/-}, IL12p40^{-/-}, IFN- γ R^{-/-}, and IFN- γ ^{-/-} mice. MHCII expression was decreased in CAFs of IL-12-deficient mice and severely impaired in those of IFN- γ /IFN- γ R-deficient versus wild-type mice (Fig. 2 B).

To probe the contribution of the tumor microenvironment in sustaining MHCII in fibroblasts, we developed an in vitro model system where we sorted PDGFR α ⁺Podoplanin⁺ fibroblasts from LLC^{mCherry} tumors and cultured them in vitro. Although by day 3 all cultured CAFs had lost MHCII, exposure to fresh lung tumor, but not to healthy lung homogenates, restored MHCII expression (Fig. 2 C). It should be noted that MHCII induction was observed upon three-dimensional (3D) but not 2D culture conditions, consistent with previous observations that 2D cultures

Supplemental material

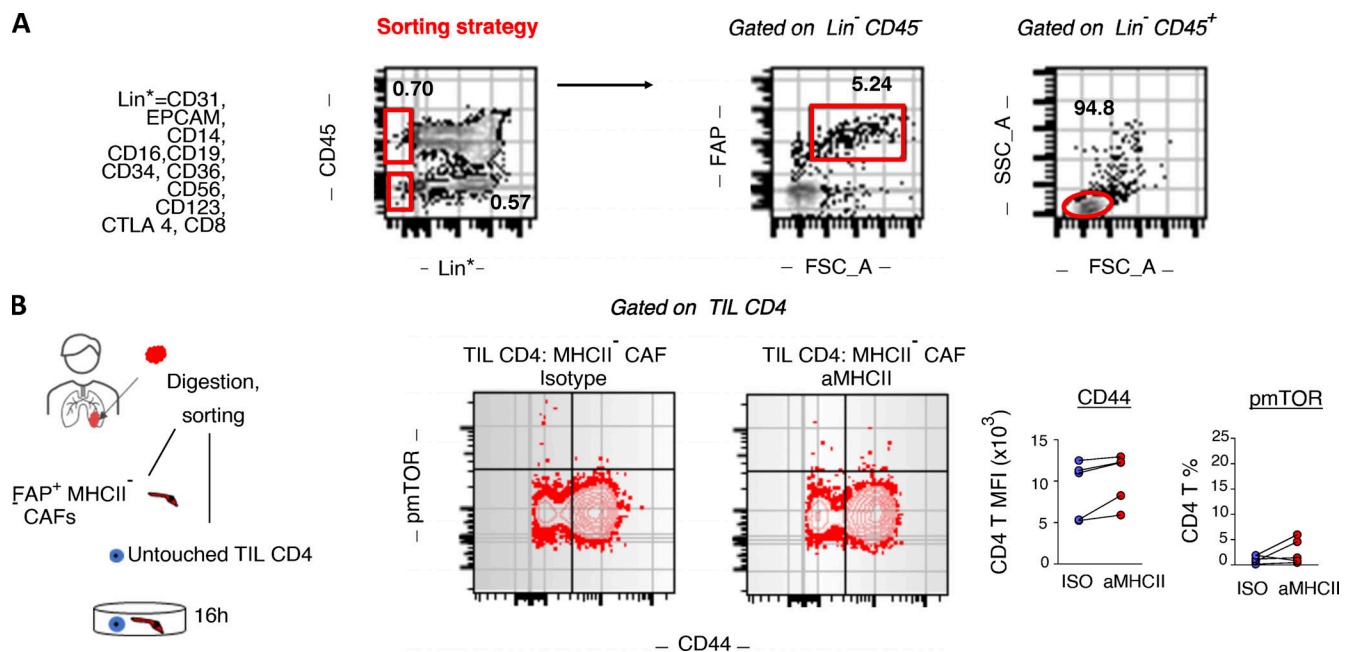


Figure S1. **Human MHCII⁻ CAF-tumor infiltrating CD4 T cell co-cultures.** (A) Gating strategy for sorting untouched CD4 T cells and CAFs from the same tumor fragment. CAFs are sorted as live FSC-A^{high}Lin⁻CD45⁻FAP⁺ and untouched CD4 T cells as FSC-A^{low}Lin⁻CD45⁺. (B) Purified CD4 T cells and FSC-A^{high}Lin⁻CD45⁻FAP⁺MHCII⁻ CAFs were co-cultured with panMHCII-blocking antibody or isotype (ISO) control. Representative FACS plots and cumulative data on phospho-mTOR (pmTOR) and CD44 ($n = 5$ patients). *, $P < 0.05$; **, $P < 0.01$. Error bars, mean \pm SEM; two-tailed paired t test. aMHCII, pan-MHCII blocking antibody; FSC-A, forward scatter-A; MFI, mean fluorescence intensity; SSC-A, side scatter-A.

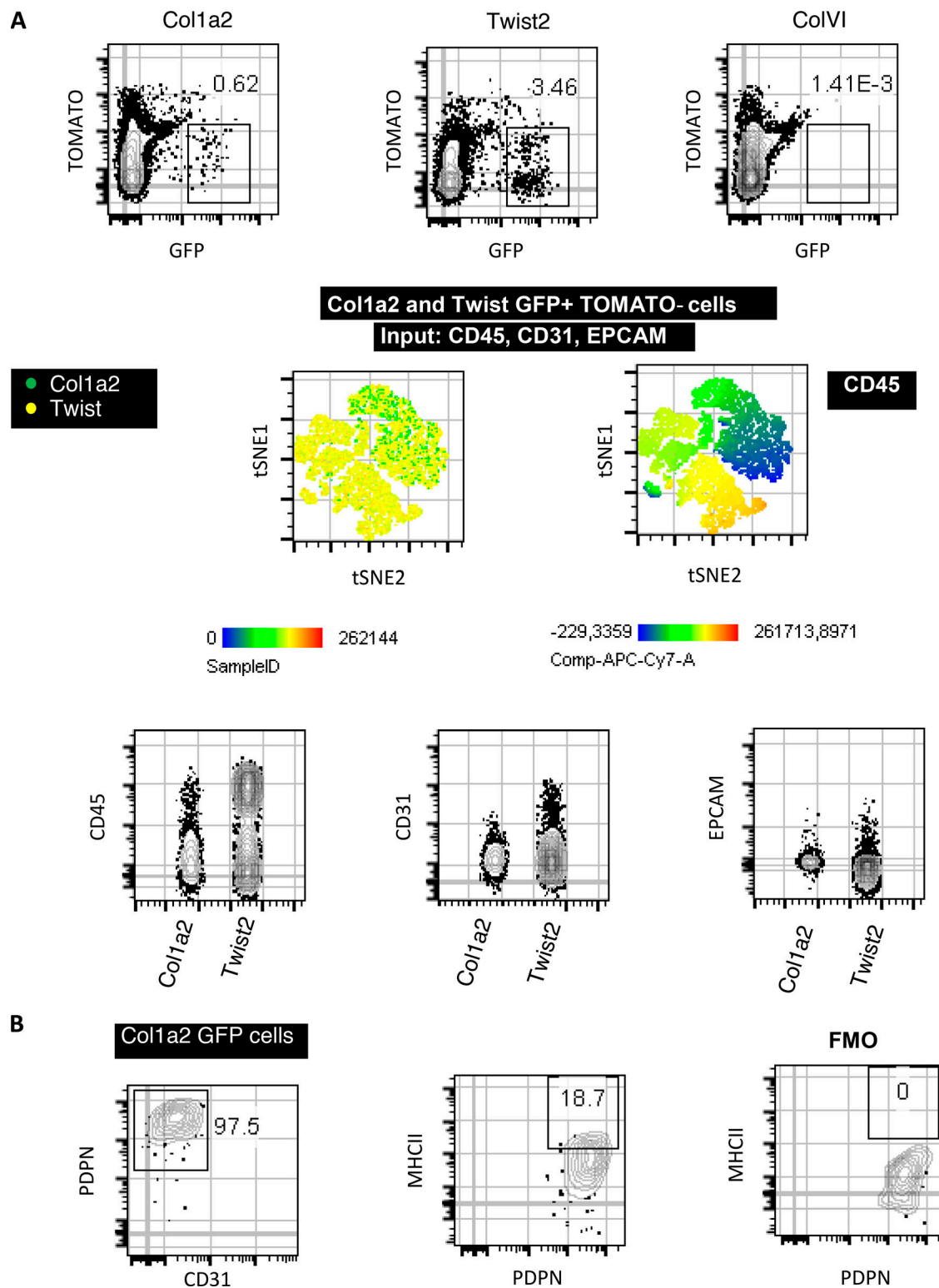


Figure S2. **Lung CAF specificity of the Col1a2-CreER, ColVI-Cre, and Twist2-Cre mouse strains.** (A and B) LLC cells were implanted intrapulmonary in the left lung lobe of tamoxifen-treated Col1a2-CreER/mTmG (Col1a2), ColVI-Cre/mTmG (ColVI), and Twist2-Cre/mTmG mice (Twist) mice. Lung tumors were digested and subjected to FACS analyses. (A) Expression of hematopoietic- (CD45), endothelial- (CD31), and epithelial- (EPCAM) specific markers by lung GFP cells. (B) Twist2 expression of the fibroblast-specific marker Podoplanin and of IAb (MHCII) ($n = 2$ per group, from two independent experiments). FMO, fluorescence minus one.

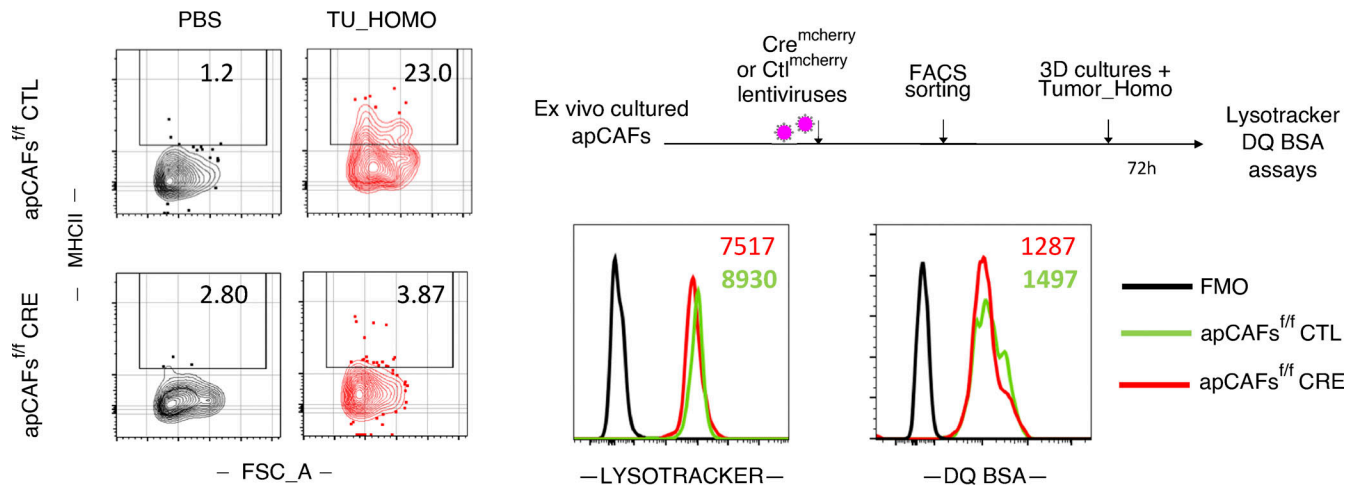


Figure S3. **Lysosomal processes of MHCII-deleted apCAFs.** Purified apCAFs from I-Ab-*fl/fl* mice were expanded and transduced with CRE^{mcherry} or control (CTL) lentiviruses. To induce MHCII, apCAFs were exposed for 72 h in 3D conditions to 30% tumor homogenate (Tumor_Homo). Left: Representative FACS plots of MHCII. Lysosomes were tracked (LysoTracker), and lysosomal proteolysis was assessed (DQ Green BSA) with FACS. Right: Representative FACS plots. FSC-A, forward scatter-A; FMO, fluorescence minus one.

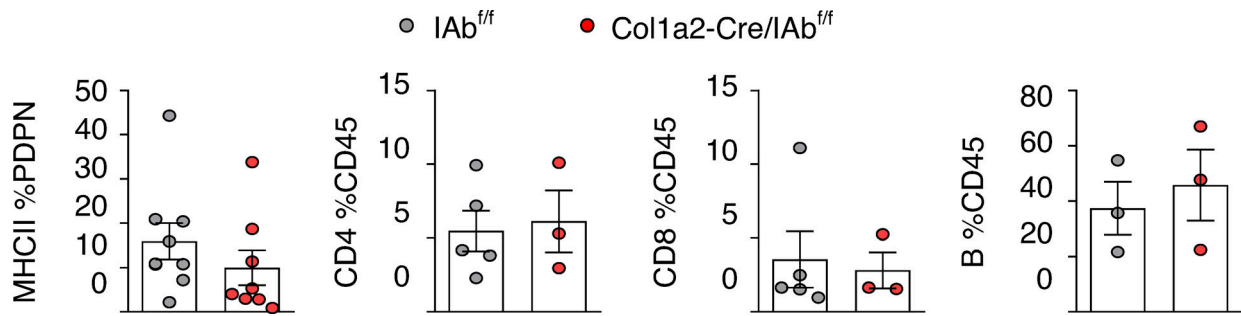


Figure S4. **FACS analysis of tumor-draining LNs of the Col1a2-CreER strain.** LLC cells were implanted intrapulmonary in the left lung lobe of Col1a2-CreER⁺I-Ab^{fl/fl} and I-Ab^{fl/fl} mice. After 14 d, mesothoracic/tumor-draining LNs were digested and analyzed by FACS. From left to right: MHCII expression in CD45⁺CD31⁺EpCAM⁺Podoplanin⁺. Frequencies of CD4⁺, CD8⁺ T cells, and B220⁺ B cells. *n* = 3–5 per group, pulled from two independent experiments. Error bars, mean ± SEM.

Table S1 is provided online and lists main patient data, including number of patients enrolled in the study, age, gender, histology, smoking history, and TNM stage.